Provided for non-commercial research and education use.
Not for reproduction, distribution or commercial use.

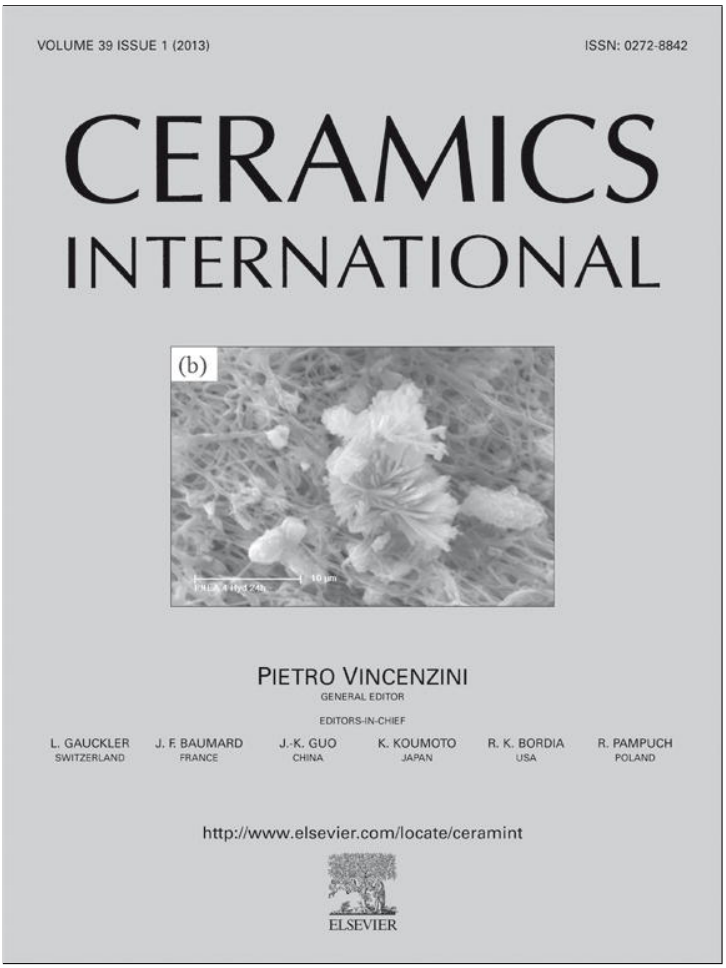

This article appeared in a journal published by Elsevier. The attached copy is furnished to the author for internal non-commercial research and education use, including for instruction at the authors institution and sharing with colleagues.

Other uses, including reproduction and distribution, or selling or licensing copies, or posting to personal, institutional or third party websites are prohibited.

In most cases authors are permitted to post their version of the article (e.g. in Word or Tex form) to their personal website or institutional repository. Authors requiring further information regarding Elsevier's archiving and manuscript policies are encouraged to visit:

http://www.elsevier.com/copyright

Author's personal copy

Available online at www.sciencedirect.com

SciVerse ScienceDirect

Ceramics International 39 (2013) 683–689

CERAMICS INTERNATIONAL

www.elsevier.com/locate/ceramint

Synthesis and characterization of partially crystalline nanosized ZSM-5 zeolites

Mohamed Mokhtar M. Mostafa*, Katabathini Narasimha Rao, Huda S. Harun, Sulaiman N. Basahel, Islam H. Abd El-Maksod

Chemistry Department, Faculty of Science, King Abdulaziz University, Jeddah 21589, P.O. Box 80203, Saudi Arabia

Received 16 March 2012; accepted 26 June 2012
Available online 1 July 2012

Abstract

Partially crystalline nanosize ZSM-5 with high surface area (678 m^2/g) was synthesized successfully without using organic template by a two-step temperature process. Aluminum nitrate was used as aluminum source for the first time to synthesize ZSM-5 materials. The presence of MFI structure of the materials was analyzed by XRD, FTIR, Raman spectroscopy and TEM techniques. Addition of commercial HZSM-5 as a seeding agent to the reactants resulted an increase in crystallinity of the ZSM-5 sample and subsequent decrease in specific surface area. The partially crystalline samples exhibited low microporosity and remarkably high meso/macropore volume with pore diameters around 30 nm.
© 2012 Elsevier Ltd and Techna Group S.r.l. All rights reserved.

Keywords: A. Powders: chemical preparation; B. Electron microscopy; B. Porosity; B. X-ray methods

1. Introduction

Zeolites occur naturally as minerals, and are extensively mined in many parts of the world. Others are synthetic, and are made commercially for specific uses, or produced by research scientists trying to understand more about their chemistry because of their unique porous properties [1]. Zeolites are used in a variety of applications with a global chemical and petrochemical industry. The major uses are in petrochemical cracking, ion-exchange (water softening and purification), and in the separation and removal of gases and solvents [2].

Zeolites have the ability to act as catalysts for chemical reactions which take place within their internal cavities. An important class of reactions is that catalyzed by hydrogen-exchanged zeolites, whose framework-bound protons give rise to very high acidity. This is exploited in many organic reactions, including crude oil cracking, isomerization and fuel synthesis [3]. Zeolites can also serve as oxidation or reduction catalysts, often after metals have been introduced into the framework. Examples are the use of Ti-ZSM-5 in the production of caprolactam, and Cu zeolites in NO*x* decomposition [4]. Underpinning all these types of reaction is the unique microporous nature of zeolites, where the shape and size of a particular pore system exerts a great influence on the reaction, controlling the access of reactants and products. Increasingly, attention has focused on fine-tuning the properties of zeolite catalysts in order to carry out very specific syntheses of high-value chemicals [5]. The microporous character of the zeolite limits the diffusion of molecules to internal catalytic sites, particularly when the diffusion in the micro-pores is significantly slower than the reaction, particularly, when the reactions are performed in the liquid phase, which adversely affect catalytic performance [6]. To overcome this problem, several novel materials such as ultra large micropore zeolite [7], ordered mesoporous zeolites [8], and zeolite nanocrystals [9] were synthesized.

Nano-sized zeolites have received much interest due to their properties of high external surface area, more exposed active sites as well as reduction of diffusion path length for substrate in catalysis. Crystal size can be

*Corresponding author. Tel.: +966 500558045; fax: +966 26952292.
E-mail addresses: mmokhtar2000@yahoo.com, mmoustafa@kau.edu.sa (M.M.M. Mostafa).

0272-8842/$36.00 © 2012 Elsevier Ltd and Techna Group S.r.l. All rights reserved.
http://dx.doi.org/10.1016/j.ceramint.2012.06.079

Author's personal copy

decreased by modifying synthesis parameters such as the gel composition or crystallization temperature. Although template synthesis of zeolite nanocrystals is a common practice, usage of templates cause many disadvantages including high cost, contamination of water by organic template agents, air pollution arising from thermal decomposition of organic templates, and coke deposit due to decomposition [10]. In order to overcome these disadvantages, researchers explored the synthesis of zeolites in absence of organic template [11]. Grose and Flanigen [12] reported the synthesis of organic-free ZSM-5 without seeding agent at 200 °C for the first time. There are many other reports followed after this report, for instance reports by Schwieger et al. [13] and Sun et al. [14].

Jacobs et al. [15] reported the existence of X-ray amorphous ZSM-5, which contained crystals of less than 8 nm size in an amorphous matrix of silica. Later, Nicolaides [16] reported the synthesis of substantially amorphous or partially crystalline zeolitic materials. He used template hydrogels for the synthesis of ZSM-5 samples at various temperatures and under autogenous pressure. He also reported that the samples synthesized at temperatures range of 25–70 °C showed X-ray amorphous nature, whereas treatment at 90 °C produced material exhibiting only 2% XRD crystallinity. More interestingly, the amorphous samples produced the highest yield of isobutene in the skeletal isomerization of 1-butene, whereas an increase in the relative crystallinity of the materials led to higher conversion values and to significantly lower selectivities to isobutene. Triantafyllidis et al. [17] reported the hydrothermal synthesis of X-ray amorphous and low-crystalline samples at temperature as low as 25 °C. The authors observed that the materials consisted of nanosized well-formed particles of almost spherical shape and with dimensions of about 20–30 nm. Corma and Daíz-Cabañas [18] also synthesized amorphous zeolites using self-assembling of organic structure directing agents. Significant efforts have been made to synthesize amorphous or partially crystalline ZSM-5 without seeding agent [19]. Partially crystalline or amorphous ZSM-5 material was successfully synthesized in absence of template or seeding agent using two-step temperature technique by Kim and Kim [20]. Recently, a modified method for the synthesis of an amorphous ZSM-5 has been reported by Yeong et al. [21].

In the present paper, we are reporting the hydrothermal synthesis of nanosized partially crystalline ZSM-5, with a large surface area, using aluminum nitrate as an aluminum source. To best of our knowledge, the application of aluminum nitrate as precursor to synthesize ZSM-5 nanomaterial has not previously been reported.

2. Materials and methods

All ZSM-5 samples are prepared by hydrothermal synthesis method using stainless steel autoclave without stirring (acid digestion vessel 125 ml, Parr instrument company, USA). The molar composition of the ZSM-5 precursor gel is (0.0159) Na_2O- (0.159) SiO_2- (0.00318) Al_2O_3- (4.77) H_2O. Aluminum nitrate nona-hydrate [$Al(NO_3)\cdot 9H_2O$, A.R. grade, Panrec Quimica] used as Al source, sodium silicate [Na_2SiO_3, A.R. grade, Panrec Quimica] as Si source and 1 M sodium hydroxide [NaOH, A.R. grade, Merck] solution was used to adjust the pH of the gels. Commercial HZSM-5 sample purchased from PQ Corporation (SiO_2/Al_2O_3=30) was used as a seeding agent.

Sample Z-I was prepared as follows; calculated amount of sodium silicate was dissolved in appropriate amount of distilled water to obtain a saturated solution. A known amount of 1 M NaOH solution was slowly added under constant stirring to the saturated solution of sodium silicate. Calculated amount of aluminum nitrate was charged into a separate beaker and dissolved in an appropriate amount of distilled water. Thereafter, the saturated aluminum nitrate solution was slowly added to the mixture of sodium silicate and sodium hydroxide solution. The contents were mixed for 1 h and subsequently HZSM-5 seeding agent was added under constant stirring at room temperature and stirring is continued for 3 h. The total contents are then transferred to a stainless steel autoclave and heated at 120 °C without stirring for 9 days. The reaction product was filtered and thoroughly washed with distilled water and dried at 100 °C for 5 h.

Z-II was prepared by following the same procedure as described above except the autoclave was left for only two days at 120 °C without stirring.

A modified method was used to synthesize Z-III sample. Two aqueous solutions of Si and Al precursors were mixed as described in Ref. [20]and then the contents were subjected to nucleation via aging process at 100 °C for one day without adding seeding agent. The solution is then transferred into Teflon coated autoclave and subjected to a two step temperature treatment without stirring. First, at 180 °C for 2 h, then cooled down to 120 °C and kept at this temperature for 24 h, after that the material is filtered and dried at 120 °C.

The phase identification for the catalysts were performed using a Philips X'pert pro diffractometer, operated at 40 kV and 40 mA, using CuKα radiation, in the 2θ range from 2° to 100° in steps of 0.02°, with a sampling time of one second/step. The average crystallite size was calculated using Scherrer's equation:

$$D = B\lambda/\left(\beta_{1/2}\cos\theta\right) \quad (1)$$

where D is the average crystallite size of the phase under investigation, B is the Scherrer's constant (0.89), λ is the wavelength of the X-ray beam used (1.54056 Å), $\beta_{1/2}$ is the full width at half maximum (FWHM) of the diffraction peak and θ is the diffraction angle. FTIR spectra were recorded in the range 300–1600 cm^{-1} on a Perkin Elmer Spectrum 100 FTIR spectrometer using KBr pellets (1 wt% zeolite in KBr matrix). Specific surface area (SSA) and porosity of the samples were determined from adsorption/desorption isotherms of nitrogen, which were

Author's personal copy

obtained at −196 °C on model Tristar 3000 automated gas sorption system (Micromeritics, USA). Prior to the determination of the adsorption isotherms, the samples were dried overnight at 150 °C. The elemental composition of the samples was measured with an Oxford EDS (Energy Dispersive Spectroscopy) detector. TEM micrographs were obtained using Phillips CM-120 instrument with lattice resolution 1.4 Å at accelerating voltage of 220 kV. Samples were fixed on carbon films supported on copper or molybdenum grids and investigated with the electron microscope. The Raman spectra of samples were measured with a Bruker Equinox 55 FT-IR spectrometer equipped with a FRA106/S FT-Raman module and a liquid N_2 cooled Ge detector, using the 1064 nm line of an Nd:YAG laser with an output laser power of 400 mW.

3. Results and discussion

Powder X-ray diffraction patterns of commercial HZSM-5, Z-I, Z-II and Z-III samples are shown in Fig. 1. The commercial HZSM-5 and Z-I sample are exhibiting diffraction peaks ranges of $2\theta = 7°–9°$ and 23°–25° corresponding to ZSM-5 structure (ICDD file no. 41-1478). This result is clearly indicating that MFI structured ZSM-5 sample can be synthesized without any template or seeding agent and also aluminum nitrate can be used as aluminum source to synthesize MFI structured zeolites. It is well known that aluminum sources can influence different aspects of MFI crystal growth, which can also lead to changes in physicochemical properties of the material. The diffraction patterns of Z-I and Z-II are majorly consisted of big hump. Appearance of small diffraction peaks on the top of the hump is observed for the samples Z-II and Z-III. The diffraction peaks are at the same degrees (2θ) as the major peaks for MFI structure. We can also observe that Z-II sample exhibiting relatively high X-ray amorphous nature than Z-I or Z-III. These observations are quite similar with the XRD results for amorphous zeolites reported by Nicolaides [16]. Van Grieken et al. [22] proved that the mechanism of ZSM-5 crystallization process under the shorter hydrothermal reaction times is different from the conventional synthesis conditions. They observed the formation of amorphous primary particles, with sizes of approximately 8–10 nm, which had undergone an aggregation process as a function of reaction time and gradually transformed into nanocrystalline ZSM-5 crystals through a zeolitization process.

The calculated lattice parameters for Z-I sample are $\alpha = 2.03$ nm, $b = 0.41$ nm and $c = 1.57$ nm. The crystallite size of this sample (20 nm) also determined using Scherrer equation. On the other hand, we could not determine the crystallite size of Z-II and Z-III samples from XRD patterns due to their amorphous nature. Jacobs et al. [15] indicated that X-ray diffraction should be used with caution for nanosized ZSM-5 amorphous materials; in contrast, they recommended I.R. technique to determine the MFI structure of this kind due to vibrations of the skeleton are intense for agglomerates of even a few unit cells.

FTIR spectra of as-synthesized samples are presented in Fig. 2. The vibrational bands were examined in the range from 300 to 1250 cm^{-1}. All the synthesized zeolites Z-I, Z-II and Z-III samples are showing a band at 550 cm^{-1}

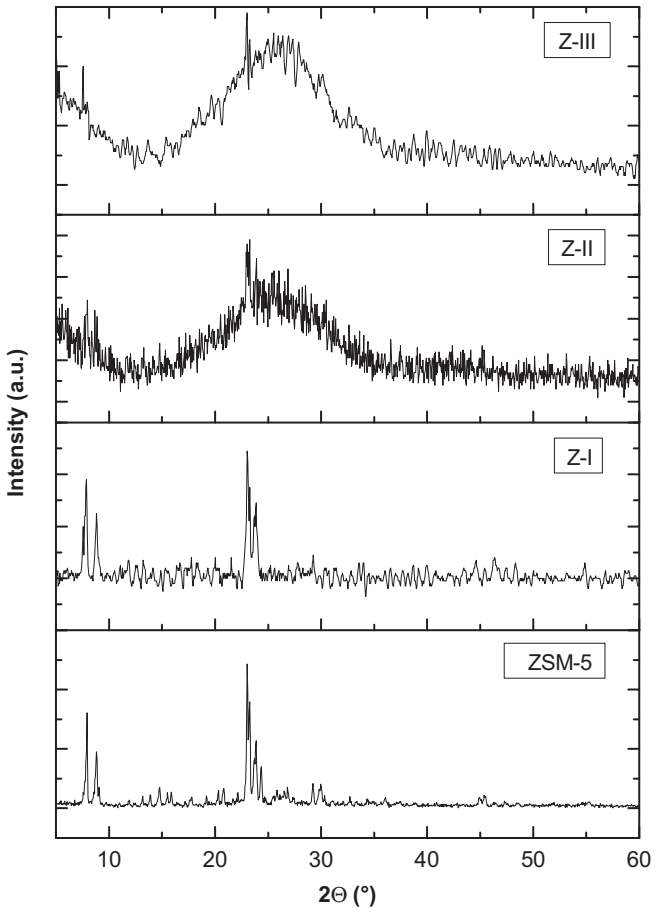

Fig. 1. XRD patterns of (a) commercial HZSM-5 (b) Z-I (b) Z-II and (c) Z-III samples.

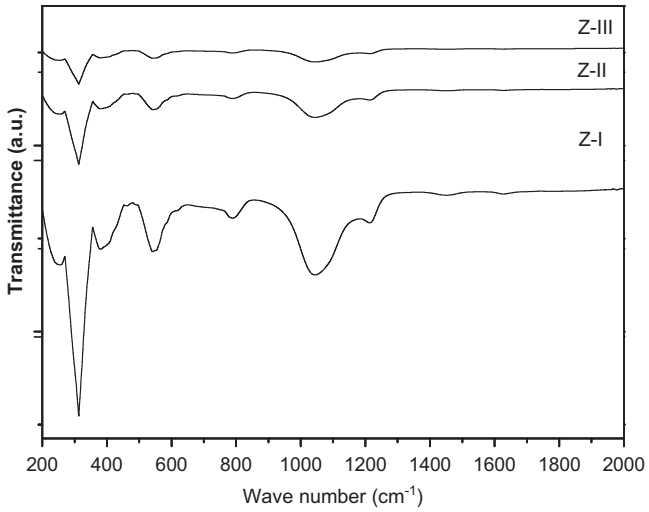

Fig. 2. FTIR spectra of (a) Z-I (b) Z-II and (c) Z-III samples.

Author's personal copy

corresponding to the MFI phase skeletal vibration [23]. This band, not observed in the amorphous silica (data not showed), is indicative of the presence of MFI atomic ordering, even in the range of a few units cells (< 8 nm) for both the samples corresponding to short synthesis times which are mostly X-ray amorphous. These results indicate the prior formation of an amorphous solid in the synthesis medium and later it turned into a crystalline ZSM-5 zeolite. This fact has also been observed by Van Grieken et al. [22] and other researchers. The intensity of characteristic band due to pentasil structure at 550 cm^{-1} is very small in the case of Z-III than Z-I and Z-II samples. Additional evidence for ZSM-5 zeolite was the peak/shoulder due to asymmetric stretch vibration of the O–T–O bond at 1200, 1195 and 1190 cm^{-1} for samples Z-I, Z-II, and Z-III, respectively. It was revealed in the literature that intensity of five-membered ring band of the ZSM-5 increases progressively with increasing synthesis time from 84 h to 216 h at 80–120 °C [9].

Chemical composition of three samples is presented in Table 1. It can be seen that the partially crystalline samples (Z-II and Z-III) have higher aluminum and sodium contents, relative to the high-crystalline Z-I samples. Presence of high sodium ions in partially crystalline samples could be due to entrapment of some sodium ions in amorphous oligomeric Si–Al hydroxy-oxides. The chemical analyses revealed that the Si/Al ratio of the synthesized samples is in the range of 42–47. In particular, the Si/Al ratio of the Z-II and Z-III is 42 and 44, respectively. The highest Si/Al ratio, that is 47, was shown for the Z-I sample. In the latter case almost total hydrothermal conversion of the amorphous silica into ZSM-5 nano zeolite bodies was noticed. A large number of reports have been published in recent years related to the mechanism of zeolite crystallization from clear solutions [24]. In many of these works the formation of primary units with sizes below 10 nm have been detected in the earlier stages of the crystallization. Although their nature (crystalline versus amorphous) and their exact role in the crystallization mechanism (dissolution versus zeolite precursors) is still a matter of debate, it has been proposed that the zeolite crystal growth proceeds by an aggregation/densification pathway starting from nanoslabs [25].

The local structure of the as-synthesized zeolite samples was additionally studied by Raman spectroscopy. Fig. 3 presents the Raman spectra of Z-I, Z-II, and Z-III samples. The peaks of Raman spectrum in the range of 300–650 cm^{-1} are indicative of the type of silicon–oxygen rings existing in the structure of zeolite [26]. A prominent band was observed at 385 cm^{-1} in all the synthesized samples, this band was specifically assigned to the predominant five-membered rings present in this zeolite [27]. The peaks around 430 and 470 cm^{-1}corresponded to the six- and four-member rings, respectively. These peaks were in good agreement with the ZSM-5 zeolite prepared by conventional methods. In the structure of the MFI-type zeolite, continuous chains of five-member rings are connected by the four- and six member rings. The bands around at 800 and 810 cm^{-1} can be assigned to Si–OH and Si–O stretches respectively. A small broad peak at 970 cm^{-1} appeared in Z-I sample similar to amorphous silica reported in the literature [28]. This peak could be resulting from the large amount of broken Si–O–Si linkages due to the porosity of the Si–O network. In the high-frequency region, the peaks at 1040 and 1215 cm^{-1} can be assigned to non-symmetric Si–O stretching vibrations and are typical of all crystalline tetrahedral silica polymorphs.

The synthesized Z-I sample exhibited a type IV isotherm (Fig. 4), thus, the Z-I molecular sieve obtained is mesoporous. The isotherms for Z-II and Z-III samples can be considered type I, since it presents very small inflection characteristics of capillary condensation processes. Type I isotherms level off already at quite low relative pressures and are characteristic of microporous materials (and often also for materials with pore sizes on the borderline between micropores and mesopores). The textural properties,

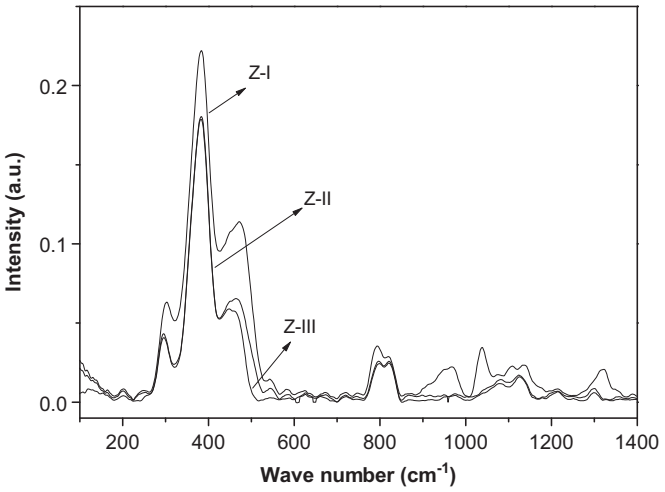

Fig. 3. Raman spectra of (a) Z-I (b) Z-II and (c) Z-III samples.

Table 1
Elemental and textural properties of the samples.

Sample name	Si/Al ratio[a]	S_{BET} (m^2/g)	S_t (m^2/g)	V_p (cc/g)	W_p (nm)
Z-I	47	434	79	0.253	2.7
Z-II	42	335	325	0.171	2.5
Z-III	44	678	354	0.344	3.6

[a]EDS elemental analysis, S_t: micro pore area, V_p: pore volume, W_p: average pore diameter.

Author's personal copy

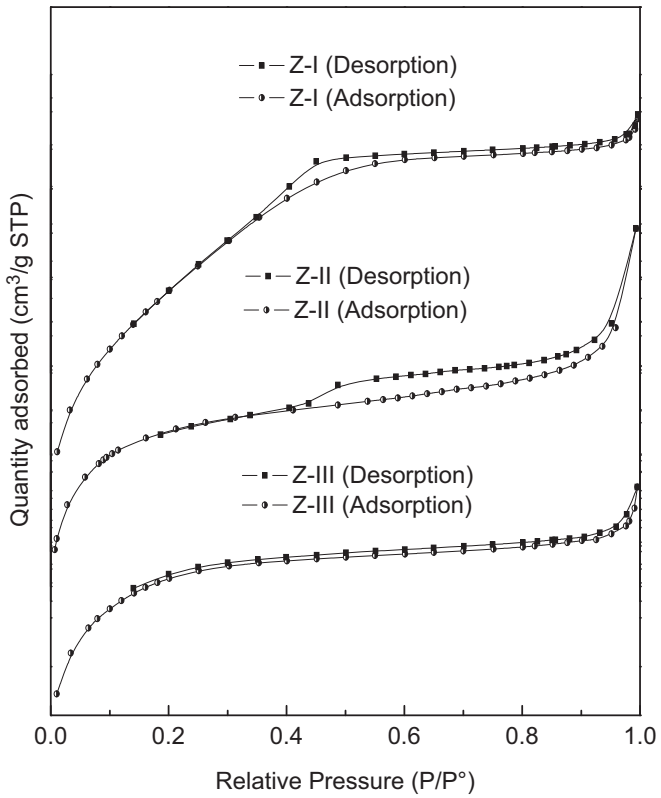

Fig. 4. Adsorption/desorption isotherms of (a) Z-I (b) Z-II and (d) Z-III samples.

namely BET specific surface area (S_{BET}), micropore area (S_t), pore volume (V_p) and average pore diameter (W_p) are presented in Table 1. The S_{BET} of Z-I is 434 m^2/g, higher than the BET-surface area of the well crystalline ZSM-5 (313 m^2/g) [29]. The increase in the external surface area could be due to the impurities of the synthesized zeolite with the amorphous silica-alumina of relatively ordered mesoporous structure [17]. The pore diameter (W_p) obtained by the BJH analysis of desorption branch of the isotherm for Z-I is about 2.7 nm (Fig. 6). However, this slight deviation from the micropore volume values (<2 nm) addressed for the presence of mesoporous material mixed with the typical microporous nanocrystalline ZSM-5. The S_{BET} of Z-II sample (335 m^2/g) and S_t (325 m^2/g) are similar to the values for nano ZSM-5 reported in the literature [30]. On the other hand, Z-III sample shows the extraordinary adsorption capacity of such materials due to enhanced adsorption in micropores. The step uptake at low relative pressure was followed by nearly horizontal adsorption and desorption branches. A second uptake at high relative pressure was also observed for this sample (Fig. 4). The upward turn with a hysteresis loop is indicative of the generated inter-crystalline mesoporosity of pore diameter (3.6 nm), which could arise due to aggregation of the nano-crystallites [31]. BET calculations showed that the surface area for this sample is 678 m^2/g, which is very high relative to the amorphous or crystalline MFI-type materials. Z-III sample also possessed pores with high micropore surface area ($\sim$345 m^2/g) and large pore volume ($\sim$0.344 cc/g). The N_2 adsorption results also indicating that there is formation of a nanocrystalline material under the described preparation conditions. This method produces materials with high micropore volume and larger external surface area (Table 1).

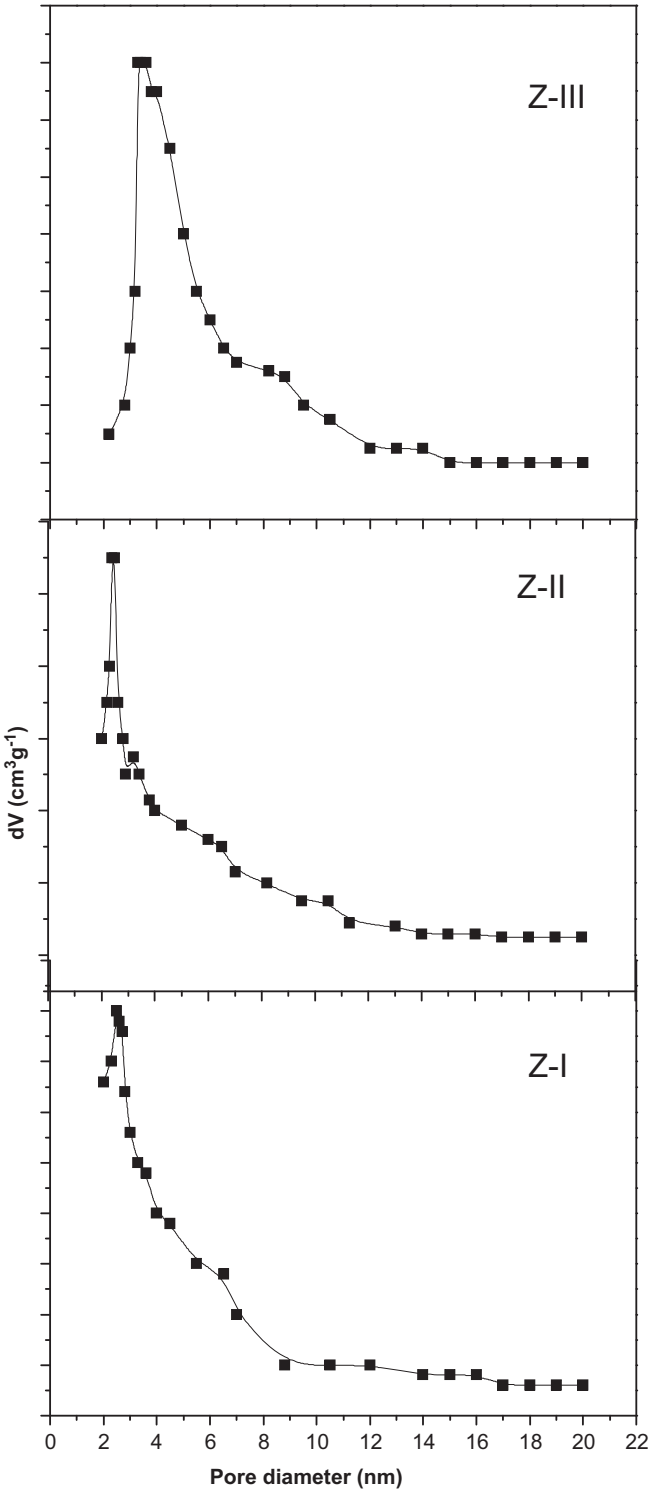

Fig. 5. Pore size distribution patterns of (a) Z-I (b) Z-II and (c) Z-III samples.

Author's personal copy

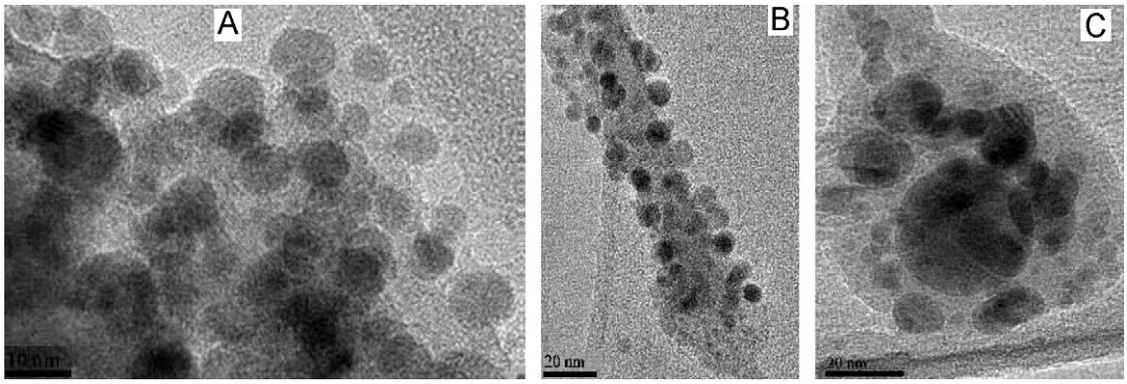

Fig. 6. TEM images of (a) Z-I, (b) Z-II and (c) Z-III samples.

The TEM images of Z-I, Z-II and Z-III are shown in Fig. 5. It is seen from the images that the zeolite particles are closely spaced, but well-separated. The characterized nanoparticles are nearly spherical with uniform particle morphology. A higher magnification result demonstrates that the particle size distribution of all samples is in the range of 10–30 nm. Among them, there exist some particles having contrasts, sizes and shapes strongly different from most zeolite particles. The particle size was also confirmed by Scherrer equation on their XRD result and the mean value of the particle size of Z-I found to be 20 nm. It is interesting to note that even the partially crystalline samples Z-II and Z-III consist of small well-formed particles of a nearly spherical shape and dimensions of 15–25 nm. The high external surface area of the low-crystallinity materials can thus be explained by the presence of these small particles which are, however, not small enough or appropriately interconnected in order to generate inter particle ordered mesoporosity, as was previously shown by Van Grieken et al. [22]. These results are remarkable as the crystallites synthesized here are much smaller than those typically obtained by the different methods reported in the literature for the preparation of nanocrystalline ZSM-5. The significant differences of crystallite size of the synthesized materials from the literature reports must be related to the variation of the synthesis conditions used in the present work, which in turn may influence and change the crystallization process. Persson et al. [32] reported that Na^+ cation plays a structural directing role in place of organic template, enhancing the nucleation, forming smaller crystals. Cheng et al. [9] indicated that adding a certain amount of Na^+ cation can stimulate the growth of zeolite crystals. Shin et al. [33] also observed that the crystal size of the zeolite was decreased with the increase of Na_2O content.

4. Conclusions

In the present study partially crystalline nano ZSM-5 zeolites were synthesized using aluminum nitrate as Al source for the first time. The different factors influencing the type, crystal structure, morphology and textural properties were studied to understand mechanism of formation of partially crystalline nano ZSM-5 materials. The modified method of preparation of ZSM-5 has a great advantage to synthesize nanosize ZSM-5 with high BET-surface area, which could influence catalyst performance in some reactions.

Acknowledgments

Mrs. H.S. Harun would like to grateful acknowledge the King Abdulaziz City for Science and Technology (KACST) for the fund no. GSP-18-132. Dr. Abdulaziz Bagabas is gratefully acknowledged for his valuable support.

References

[1] H. Van Bekkum, E.M. Flanigen, J.C. Jensen, Introduction to Zeolite Sciences and Practice, first ed., Elsevier, Amsterdam, 1991.
[2] B.C. Gates, Catalytic Chemistry, first ed., John Wiley & Sons, New York, 1991.
[3] E.H. Teunissen, A.P. Jansen, R.A Van Santen, R. Orlando, R. Dovesi, Adsorption energies of NH_3 and NH_4^+ in zeolites corrected for the long-range electrostatic potential of the crystal, Journal of Chemical Physics 101 (1994) 5865–5874.
[4] G. Li, S. Larsen, H.V. Grassian, Catalytic reduction of NO_2 in nanocrystalline NaY zeolite, Journal of Molecular Catalysis A: Chemical 227 (2005) 25–35.
[5] H. Van Bekkum, R. Sheldon, Fine Chemicals Through Heterogeneous Catalysis, first ed., Wiley-VCH, New York, 2001.
[6] D. Bruhwiler, G. Calzaferri, Molecular sieves as host materials for supramolecular organization, Microporous and Mesoporous Materials 72 (2004) 1–3.
[7] J.H. Clark, C.N. Rhodes, Clean Synthesis Using Porous Inorganic Solid Catalysts and Supported Reagents, first ed., R.S.C., Cambridge, 2000.
[8] A. Corma, State of the art and future challenges of zeolites as catalysts, Journal of Catalysis 216 (2003) 298–312.
[9] Y. Cheng, L.J. Wang, J.S. Li, Y.C. Yang, X.Y. Sun, Preparation and characterization of nanosized ZSM-5 zeolites in the absence of organic template, Materials Letters 59 (2005) 3427–3430.
[10] D. Hu, Q.H. Xia, X.H. Lu, X.B. Luo, Z.M. Liu, Synthesis of ultrafine zeolites by dry-gel conversion without any organic additive, Materials Research Bulletin 43 (2008) 3553–3561.
[11] S. Stefan, M. Thomas, L.F. John, D.N. Richard, Transport of Q isomers through ZSM-5 zeolite membranes, Journal of Membrane Science 224 (2003) 51–67.

Author's personal copy

[12] R.W. Grose, E.M. Flanigen, Crystalline Silica, US patent no. 4061724, 1977.
[13] W. Schwieger, K.H. Bergk, D. Hunger, H. Pfeifer, Synthesis of pentasil zeolites with and without organic templates, in: M.L. Occelli, H.E. Robson (Eds.), Zeolite Synthesis, ACS symposium series, Washington, DC, 1989, pp. 274–290.
[14] S.H. Sun, J.T. Ma, X.H. Gao, Synthesis of ZSM-5 on kaolin microspheres in the absence of an organic amine template, Clay Minerals 42 (2007) 203–211.
[15] P.A. Jacobs, E.G. Derouane, J. Weitkamp, Evidence for x-ray-amorphous Zeolites, Journal of the Chemical Society Chemical Communications 12 (1981) 591–593.
[16] C.P. Nicolaides, A novel family of solid acid catalysts: substantially amorphous or partially crystalline zeolitic materials, Applied Catalysis A: General 185 (1999) 211–217.
[17] K.S. Triantafyllidis, L. Nalbandian, P.N. Trikalitis, A.K. Ladavos, T. Mavromoustakos, C.P. Nicolaides, Structural, compositional and acidic characteristics of nanosized amorphous or partially crystalline ZSM-5 zeolite-based materials, Microporous and Mesoporous Materials 75 (2004) 89–100.
[18] A. Corma, M.J. Díaz-Cabañas, Amorphous microporous molecular sieves with different pore dimensions and topologies: synthesis, characterization and catalytic activity, Microporous and Mesoporous Materials 89 (2006) 39–46.
[19] N.Y. Kang, B.S. Song, C.W. Lee, W.C. Choi, K.B. Yoon, Y.K. Park, The effect of Na_2SO_4 salt on the synthesis of ZSM-5 by template free crystallization method, Microporous and Mesoporous Materials 118 (2009) 361–372.
[20] W.J. Kim, S.D. Kim, Method of Preparing ZSM-5 Using Variable Temperature Without Organic Template, US Patent no. 7,361,328 B2, 2008.
[21] Y.F. Yeong, A.Z. Abdullah, A.L. Ahmed, S. Bhatia, Propylsulfonic acid functionalized partially crystalline silicalite-1 materials: synthesis and characterization, Journal of Porous Materials 18 (2001) 147–157.
[22] R. Van Grieken, J.L. Sotelo, J.M. Menendez, J.A. Melero, Anomalous crystallization mechanism in the synthesis of nanocrystalline ZSM-5, Microporous and Mesoporous Materials 39 (2000) 135–147.
[23] S.L. Burkett, M.E. Davis, Mechanism of structure direction in the synthesis of Si-ZSM-5: an investigation by intermolecular ^{1}H–^{29}Si CP MAS NMR, Journal of Physical Chemistry B 98 (1994) 4647–4653.
[24] D.P. Serrano, J. Aguado, G. Morales, J.M. Rodríguez, A. Peral, M. Thommes, J.D. Epping, B.F. Chmelka, Molecular and meso- and macroscopic properties of hierarchical nanocrystalline ZSM-5 zeolite prepared by seed silanization, Chemistry of Materials 21 (2009) 641–654.
[25] D.P. Serrano, R. Van Grieken, Heterogenous events in the crystallization of zeolites, Journal of Materials Chemistry 11 (2001) 2391–2407.
[26] Q. Li, B. Mihailova, D. Creaser, J. Sterte, Aging effects on the nucleation and crystallization kinetics of colloidal TPA-silicalite-1, Microporous and Mesoporous Materials 43 (2001) 51–59.
[27] P.K. Dutta, K.M. Rao, J.Y. Park, Correlation of Raman spectra of zeolites with framework architecture, Journal of Physical Chemistry 95 (1991) 6654–6656.
[28] P.P. Knops-Gerrits, D.E. De Vos, E.J.P. Feijen, P.A. Jocobs, Raman spectroscopy on zeolites, Microporous Materials 8 (1997) 3–17.
[29] P. Wang, B. Shen, J. Gao, Synthesis of ZSM-5 zeolite from expanded perlite and its catalytic performance in FCC gasoline aromatization, Catalysis Today 125 (2007) 155–162.
[30] P. Wang, B. Shen, D. Shen, T. Peng, J. Gao, Synthesis of ZSM-5 zeolite from expanded perlite/kaolin and its catalytic performance for FCC naphtha aromatization, Catalysis Communications 8 (2007) 1452–1456.
[31] G. Majano, A. Darwiche, S. Mintova, V. Valtehev, Seed-Induced crystallization of nanosized Na-ZSM-5 crystals, Industrial & Engineering Chemistry Research 48 (2009) 7084–7091.
[32] A.E. Persson, B.J. Schoeman, J. Sterte, J.E. Otterstedt, Synthesis of stable suspensions of discrete colloidal zeolite (Na, TPA)ZSM-5 crystals, Microporous and Mesoporous Materials 15 (1995) 611–619.
[33] D.K. Shin, H.N. Shi, H.S. Kyeong, J.K. Wha, Compositional and kinetic study on the rapid crystallization of ZSM-5 in the absence of organic template under stirring, Microporous and Mesoporous Materials 72 (2004) 185–192.